Detection of Vegetation Changes Associated with Extensive Flooding in a Forested Ecosystem

William K. Michener and Paula F. Houhoulis

Abstract

Monitoring broad-scale ecological responses to disturbance can be facilitated by automated change-detection approaches using remotely sensed data. This study evaluated the effectiveness of five unsupervised change-detection techniques using multispectral, multitemporal SPOT High Resolution Visible (HRV) data for identifying vegetation responses to extensive flooding of a forested ecosystem associated with Tropical Storm Alberto in July 1994. Standard statistical techniques, logistic multiple regression, and a probability vector model were used to quantitatively and visually assess classification accuracy.

The change-detection techniques were (1) spectral-temporal change classification, (2) temporal change classification based on the Normalized Difference Vegetation Index (NDVI), (3) principal components analysis (PCA) of spectral data, (4) PCA of NDVI data, and (5) NDVI image differencing. Spectral-temporal change classification was the least effective of the techniques evaluated. Classification accuracy improved when temporal change classification was based on NDVI data. Both PCA methods were more sensitive to flood-affected vegetation than the temporal change classifications based on spectral and NDVI data. Vegetation changes were most accurately identified by image differencing of NDVI data. Logistic multiple regression and a probability vector model were especially useful for relating spectral responses to vegetation changes observed during field surveys and identifying areas of agreement and disagreement among the different classification methods.

Introduction and Objectives

Hurricanes and tropical storms, like other large natural disturbances, play an important role in regulating ecosystem structure and function, as well as affecting diverse plant and animal populations and communities (Pickett and White, 1985; Loope *et al.* 1994; Michener *et al.*, 1997). Because vegetation typically exhibits abrupt changes in physiognomy and spectral characteristics in response to acute disturbances, environmental scientists are increasingly using remotely sensed data to detect these changes over broad spatial and spectral scales. Change-detection analyses, employing satellite data obtained prior to and following a disturbance, have been used to assess vegetation responses to drought (Peters *et al.*, 1993; Jacobberger-Jellison, 1994), insect outbreaks (Muchoney and Haack, 1994), dust storms (Chavez and MacKinnon, 1994), high winds (Cablk *et al.*, 1994; Johnson, 1994), deforestation (Foody and Curran, 1994), and other disturbances.

Tropical Storm Alberto presented a unique opportunity to utilize satellite data to assess vegetation responses to flooding in a forested ecosystem and to compare analytical approaches for vegetation change detection. Minimal wind and storm surge damage accompanied Alberto as it made landfall on the Florida panhandle near Fort Walton Beach on 3 July 1994 and traveled inland. However, due to weak steering currents, the storm remained relatively stationary over southwestern Georgia and southeastern Alabama. Over a period of six days (2-7 July 1994), one-third of Georgia and one-sixth of Alabama recorded over 17 cm of precipitation (Garza, 1995). Rainfall was especially heavy (up to 53 cm) in the Flint and Ocmulgee River basins in southwestern Georgia, and flood discharges in tributaries and mainstems of the two rivers exceeded 100-year flood discharges along most stream reaches (Stamey, 1995). Flood discharges inundated riparian habitats, as well as agricultural fields, pine plantations, and upland habitats adjacent to streams and rivers. Natural terrestrial habitats in the flood-affected area are primarily characterized by longleaf pine (*Pinus palustris*) and wiregrass (*Aristida stricta*), the dominant ground cover species.

Various analytical approaches differing in mathematical complexity, processing and analysis intensity, classification technique, and interpretability have been used to detect vegetation change. Dobson *et al.* (1995a) reviewed several image processing techniques that used Landsat Thematic Mapper (TM) data for coastal change detection. Many studies have relied upon less computationally intensive post-classification change-detection techniques using images from one or two dates (Aldrich, 1975; Sirois and Ahern, 1989; Dobson *et al.*, 1995b; Olsson, 1995). Recently, principal components analysis (PCA), various vegetation indices, and logic rules have been implemented utilizing multitemporal satellite data (Bauer *et al.*, 1994; Muchoney and Haack, 1994; Jensen *et al.*, 1995; Walsh and Townsend, 1995). Muchoney and Haack (1994), for example, evaluated four supervised change-detection approaches using multitemporal SPOT HRV data, ranging from standard post-classification change detection to more analytically complex image differencing and PCA techniques, for identifying hardwood forest defoliation caused by gypsy moth infestation. In their study, overall accuracy ranged from 0.61 (post-classification, spectral-temporal) and 0.63 (PCA) to 0.69 (image differencing) relative to traditional air survey approaches to monitoring defoliation.

Increased interest in climate change, changing land-use

Joseph W. Jones Ecological Research Center, Rt. 2, Box 2324, Newton, GA 31770.

Photogrammetric Engineering & Remote Sensing, Vol. 63, No. 12, December 1997, pp. 1363–1374.

0099-1112/97/6312-1363$3.00/0

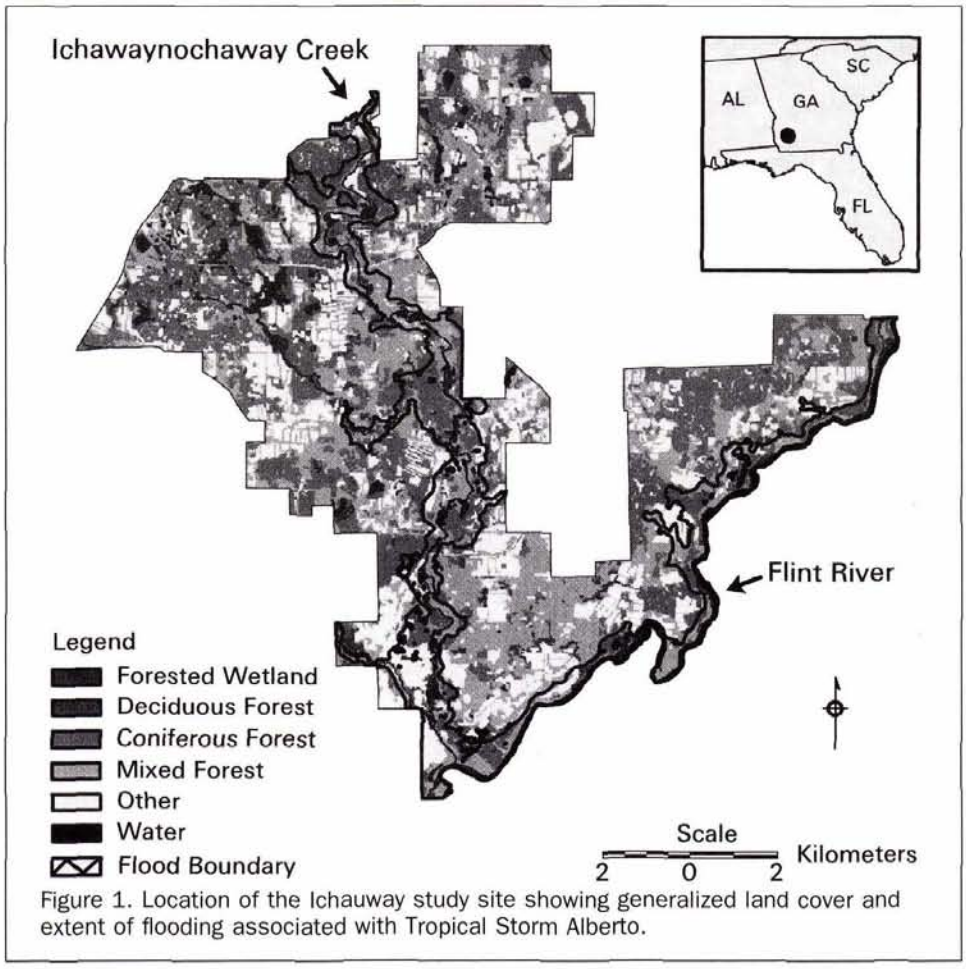

Figure 1. Location of the Ichauway study site showing generalized land cover and extent of flooding associated with Tropical Storm Alberto.

patterns, and natural and anthropogenic disturbances, coupled with high labor costs and difficulty in synoptically sampling large areas, have led to increased reliance on remotely sensed data and digital image change-detection techniques for documenting changes in ecological structure and function at broad spatial scales. Although it is generally possible to *a priori* identify relevant data sources, the selection of a single change-detection method to address a specific problem may not be a straightforward task (Collins and Woodcock, 1996). For example, vegetation and related spectral responses to a disturbance may vary markedly by type and intensity of disturbance, ecosystem type, and other environmental factors. Some change-detection techniques may therefore be more appropriate for specific types of changes and ecosystems. Most studies reported in the literature document the use of a single method for a specific problem and do not offer direct comparisons with other possible methods (but see Muchoney and Haack (1994)). Furthermore, change-detection techniques are often not well developed or widely applied and algorithms are not well tested in a variety of ecosystem types (Cohen *et al.*, 1996). Consequently, analysts have been encouraged to employ and compare a variety of supervised and unsupervised methods for their applicability to a particular problem (Dobson *et al.*, 1995a).

The purpose of this study was to compare five unsupervised change-detection approaches for their ability to discriminate vegetation responses to differential severity of flooding using SPOT HRV data. Relatively sparse overstory canopy coverage in longleaf pine-dominated stands, typical of many forest savannas that occur throughout the world, enabled SPOT's high resolution satellite sensors to detect spectral characteristics of the dense ground cover vegetation. Extensive ground surveys supported evaluation of the effectiveness of different change-detection approaches. In addition to standard statistical accuracy assessment procedures, two other procedures were used to quantitatively and visually compare the five change-detection methods. First, logistic multiple regression was used for relating spectral responses to observed vegetation changes (percent dead and percent live) and magnitude of flood disturbance. Second, probability vector modeling (PVM) was used for identifying areas of agreement and disagreement among the different classification methods.

The importance of this study was to show that SPOT HRV data and appropriate change-detection analyses can be used to monitor responses of natural vegetation communities to disturbances such as flooding. Logistic multiple regression and PVM represent two relatively new techniques that could significantly enhance our understanding of the relationship between environmental change and spectral variability, as well as facilitate the design of ground surveys and selection of appropriate change-detection methods. Use of this technology in other regionally important ecosystems will increase our understanding of how spectral patterns and variation, and ecosystem structure and function are affected by natural disturbances.

Study Area

Ichauway is a 115 km^2 ecological reserve that is located in Baker County in southwest Georgia, 45 km southwest of Albany (Figure 1). The site is located along the Flint River at its confluence with Ichawaynochaway Creek. Approximately

22 km of Ichawaynochaway Creek and 19 km of the Flint River, a brownwater stream originating in the Georgia Piedmont region, are located within the reserve. The riparian zone for both Ichawaynochaway Creek and the Flint River is very constricted and consists of two principal geomorphic components, seasonally flooded hardwood hammocks and longleaf pine-dominated upland terraces. Flood tolerant species are confined to hardwood hammocks (200 ha) or steep banks adjacent to terraces (Figure 1). Generally, flow in Ichawaynochaway Creek and the Flint River is low and stable from early summer through autumn. Winter and early spring storms often result in bankfull discharges and inundation of riparian areas.

Forested upland communities comprise 7,557 ha and are dominated by longleaf pine (2,778 ha), mixed pine (423 ha; primarily longleaf pine and slash pine, *Pinus elliotti*), and mixed pines and hardwoods (3,039 ha; primarily longleaf pine and oaks, *Quercus* spp.). Other communities include mixed hardwoods (934 ha; dominated by live oak (*Q. virginiana*), laurel (*Q. hemisphaerica*), and water oak (*Q. nigra*)); deciduous mesic (222 ha, primarily American beech (*Fagus grandifolia*), Southern magnolia (*Magnolia grandiflora*), white oak (*Q. alba*), hickory (*Carya* spp.), and sweetgum (*Liquidambar styraciflua*)); deciduous xeric (70 ha; comprised of turkey (*Q. laevis*), sandpost (*Q. margaretta*), post (*Q. stellata*), bluejack (*Q. incana*), and Southern red oaks (*Q. falcata*), as well as black cherry (*Prunus serotina*) and several associated species); and cypress wetlands (91 ha; *Taxodium* spp.).

Although wiregrass is the predominant ground cover species, silkgrass (*Pityopsis graminifolia*) can be found in abandoned agriculture fields and scrub/shrub vegetation is relatively common in more xeric habitats. Historically, high productivity and plant biodiversity in longleaf pine savannas was maintained by infrequent summer fires that were initiated by lightning strikes. The natural burning regime throughout the southeastern U.S. has, however, been almost entirely supplanted by managed fires that are initiated during winter or spring on an annual or biannual basis. Forested portions of the study area generally are managed with an annual spring burn which serves to retain the open savanna conditions and reduce hardwood encroachment and midstory canopy development.

The Remotely Sensed Data

A scene acquisition request was placed with SPOT Image Corporation in late July, 1994 for a multispectral (XS) image of the study area. Due to the amount of cloud cover during the period following Tropical Storm Alberto, a satisfactory image was not obtained until 28 September 1994. Two additional SPOT-XS images (18 October 1986 and 05 October 1990), seasonally similar to the 1994 image, were acquired from the SPOT image archive. All images were processed to level 1B, were predominantly cloud-free, and had incidence angles less than 10 degrees (−0.9, −3.3, and −9.7, respectively).

When change-detection analysis is based on data acquired immediately prior to and following a discrete disturbance event, spectral change may be related to ecological changes with a reasonably high degree of certainty. Otherwise, spectral changes associated with a specific disturbance may be confounded with land-use change, annual phenological differences, climate, and other factors that differ between the pre- and post-disturbance imagery. The two pre-flood images acquired for 1986 and 1990 were observed to encompass much of the natural variability in vegetation spectral characteristics (1986 representative of dry conditions that frequently occur in the ecosystem during the fall; 1990 typical of wetter summer-fall precipitation conditions). Because land use had not changed appreciably in the study area between 1986 and 1994, an *a priori* decision was made to use both the 1986 and 1990 images as the basis for characterizing pre-flood conditions. By doing so, we were inferring that spectral changes exhibited in 1994 exceeded the variability associated with natural climatic fluctuations and likely represented ecologically significant responses to the flood.

Image Rectification

Twenty-three ground control points (GCPs) digitized from USGS 7.5-minute topographic quadrangles (USGS quads) were used to rectify the 5 October 1990 SPOT-XS image to a Universal Transverse Mercator (UTM) map projection (RMSE = ± 0.3 pixels / ± 5.9 m). The 1986 and 1994 images were rectified using GCPs obtained from the 1990 rectified image (1986 RMSE = ± 0.2 pixels / ± 4.6 m, 1990 RMSE = ± 0.3 pixels / ± 6.6 m). The images were resampled to a 20-m pixel size using a nearest-neighbor resampling technique to retain radiometric integrity (Jensen, 1986; Jensen *et al.*, 1993). To insure that the data layers used in this analysis were co-registered, the relative error between the images and the ancillary data layers was estimated by taking the difference between ten well distributed checkpoints (road intersections) whose coordinates were recorded from the rectified images and the GIS transportation layer (discussed below) (Wolter *et al.*, 1995). The relative error (RMSE) was less than ± 5 m in each case.

Image Normalization

It is important that multi-date images be normalized to minimize changes in brightness values due to detector calibration, sun angle, Earth/sun distance, atmospheric attenuation, and phase angle between dates. After scene normalization, changes in brightness values are assumed to reflect changes in surface conditions. Absolute radiometric calibration techniques require ground reflectance data, and information about the sensor and atmosphere for the date of image acquisition, which are often difficult or impossible to obtain for archived imagery (Price, 1987; Kim and Elman, 1990; Ferencz *et al.*, 1993; Olsson, 1995). In such cases, empirical normalization techniques based on linear regression models can be used to correct for relative differences in atmospheric and other non-surface conditions among multiple image dates (Schott *et al.*, 1988; Vogelmann, 1988; Caselles and Lopez-Garcia, 1989; Eckhardt *et al.*, 1990; Hall *et al.*, 1991; Jensen *et al.*, 1995).

The 5 October 1990 SPOT-XS scene was selected as the base scene to which the 1986 and 1994 scenes were normalized because aerial photographs were available for this period (discussed below). Seven radiometric normalization targets were common among all image dates and included (1) two "dark" water bodies (deep ponds), (2) three conifer forest stands, and (3) two "bright" agricultural fields (unvegetated bare soils). All targets were located in relatively flat areas, provided a consistent appearance over time, and were assumed to represent constant reflectors (Vogelmann, 1988; Eckhardt *et al.*, 1990).

Digital numbers were sampled using a 3 by 3 window, in similar areas of the normalization targets in each image. Regression equations were developed by correlating the target brightness values obtained for the scenes being normalized (1986, 1994) with the brightness values of the base image targets (1990) for each band (Table 1). The derived regression equations were applied to the 1986 and 1994 imagery, resulting in normalized datasets in which spectral variation related to atmospheric path radiance, detector calibration, sun angle, atmospheric attenuation, and phase angle between dates was minimized.

Ancillary Data Layers

Ancillary data layers were used to assess classification accuracy, characterize damage within the flood zone, and derive

other data layers such as image masks that were used in the change-detection analyses. The following sections document relevant aspects of the GIS database development, field surveys, and spatial data manipulations and analyses.

GIS Layers

GIS data layers were developed in conjunction with the Mississippi Remote Sensing Center (MRSC) at Mississippi State University, Starkville, Mississippi. Four ancillary data layers used in this study (land cover, ground cover, hydrography, and transportation) were interpreted from 1:12,000-scale color infrared (CIR) aerial photographic transparencies and field surveys. Data were transferred to USGS quads using a vertical sketchmaster, digitized, and attributed. Land-cover classification attributes included detailed descriptions of tree species composition, age class, and stand density for all forested areas. Ground-cover attributes included primary and secondary understory vegetation classes and vegetation density. The transportation layer included linear features such as fire-breaks, state and county maintained roads, and highways. To insure that the layers were co-registered, MRSC used hydrography and transportation as a coincident line layer, keeping these features consistent in each of the other photo-interpreted layers. Soils data were transferred from 1:20,000-scale Natural Resources Conservation Service soil survey sheets to USGS quads, digitized, and attributed with soil codes, soil texture, slope, and hydrologic group. Elevation spot heights and 1.52-m (5-ft) contours were digitized from USGS quads. In a few cases, 1.52-m contours were interpolated from 3.05-m (10-ft) contours.

The progression of the floodwaters was monitored on site, and maximum water levels were recorded at approximately 350 locations along Ichawaynochaway Creek and the Flint River. High water levels were surveyed with Trimble Global Positioning System (GPS) Pro XL and Basic Plus receivers and differentially corrected (± 2 m) to a known Community Base Station. Maximum water levels were used to derive a flood boundary map by overlaying the points on topography, and extrapolating along contour lines between the points to form a polygon (Figure 1).

Raster Layers

The ground-cover and land-cover layers were combined, and were used to define a mask containing only forested areas, excluding agriculture, urban areas, roads, water, non-forested wetlands, and regenerating forest stands. This process reduced the potential confusion between flood-damaged vegetation and other land uses and changes (e.g., crop rotations). The combined ground-cover and land-cover layer, as well as the transportation and flood boundary layers, were converted to raster format (20-m cell size). Elevation spot heights and lines were combined to create a triangular irregular network (TIN). The TIN was converted to raster format with a 10-m resolution. The elevation surface was then divided into parcels based on the elevation of the Flint River or Ichawaynochaway Creek, and flood zones were created at 1.52-m contour intervals above bank-full conditions. Parcels were rejoined to form a seamless layer that was used to characterize the magnitude of flooding (Plate 1). For example, Zone 1 is within 1.52 m vertical elevation of the bank and might be expected to experience the longest period of inundation and deepest flood waters. These raster layers were used along with *in situ* reference data for accuracy assessments, and as ancillary data for spatial analyses.

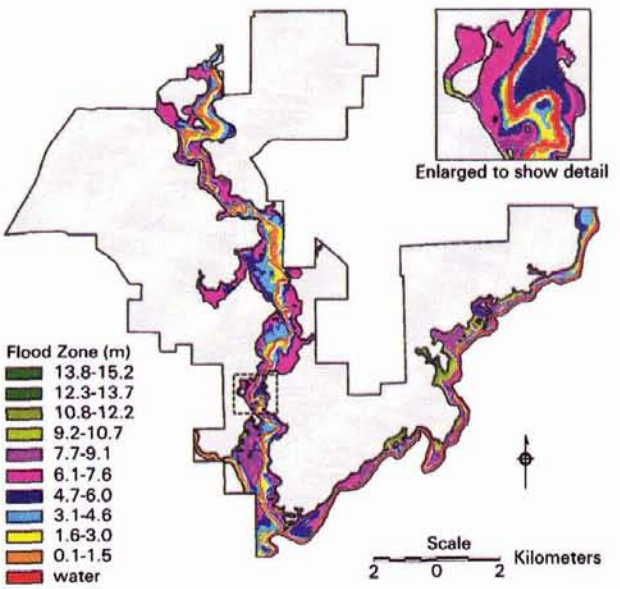

Plate 1. Zones in the flood-affected area experiencing differential severity of flooding (derived from 5-ft contours); Zone 1 is located within 1.5-m elevation of the bank and might be expected to experience the longest period of inundation, highest current velocities, and deepest flood waters.

In Situ Reference Data

One-hundred thirty-nine sites (approximately 650 m² per site) containing wiregrass and longleaf pine seedlings and saplings were surveyed throughout the flooded area to quantify vegetation damage. Data related to longleaf pine mortality were collected as part of another study and are reported in Michener *et al.* (1995). Each site contained three randomly chosen plots where ground-cover mortality was assessed using a 1-m quadrat divided into a 10 by 10 grid (10-cm intervals). Presence of bare ground, detritus, and wiregrass condition (dead, live, or recovering) were recorded at all points and the data from the three plots were averaged and converted into percentages. All sites were surveyed using the GPS techniques described earlier. One-hundred twelve of the sites coincided with the combined ground-cover/land-cover binary mask used in the remote sensing analysis and were included in accuracy assessments.

Image Classification

Several general classes of algorithms have been used to detect land-use and vegetation change, including post-classification change detection, spectral-temporal change classification (S-TCC, also known as layered temporal change classification), image differencing, image ratioing, PCA, and change vector

TABLE 1. REGRESSION EQUATIONS[1] USED TO NORMALIZE RADIOMETRIC CHARACTERISTICS OF THE 1986 AND 1994 DATA WITH THE 5 OCTOBER 1990 SPOT XS DATA

Date	Band 1 (Green)	Band 2 (Red)	Band 3 (Near Infrared)
18 Oct 86	$y = 1.23\ (x) + 2.43,\ r^2 = 0.93$	$y = 1.58\ (x) - 5.05,\ r^2 = 0.98$	$y = 1.34\ (x) - 1.32,\ r^2 = 0.93$
28 Sep 94	$y = 0.93\ (x) + 2.76,\ r^2 = 0.98$	$y = 1.02\ (x) + 0.29,\ r^2 = 0.99$	$y = 0.98\ (x) - 1.40,\ r^2 = 0.99$

[1]$P \leq 0.001$ for all models.

analysis (Jensen, 1986; Dobson *et al.*, 1995a). Three classes of algorithms (S-TCC, PCA, and image differencing) were selected for examination in this study. The algorithms were chosen for several reasons. First, analyses based on the three algorithms require only a single classification of multi-date imagery, unlike post-classification comparisons where each image must be independently classified. Second, the algorithms differ markedly in their underlying logical and statistical basis, analytical complexity, and interpretability. Third, although the three algorithms are frequently used for detecting land-use and vegetation change, few studies have employed more than one approach and little comparative information exists that can facilitate selection of the most appropriate method for a specific project (Collins and Woodcock, 1996). Fourth, two of the methods (PCA and image differencing) have been suggested to offer the greatest potential for automated mapping of vegetation change (Muchoney and Haack, 1994).

Because numerous variations exist for each algorithm, it was impractical to compare all change-detection alternatives. Five unsupervised change-detection techniques representing variations of the three generic algorithms were examined in this study. The first, spectral-temporal change classification (S-TCC), is based on unsupervised classification of spectral data from all three dates. The second approach, NDVI-TCC, requires that the Normalized Difference Vegetation Index (NDVI) be derived for each of the three dates prior to unsupervised classification. Two change-detection approaches were based on PCA, a multivariate statistical technique that isolates inter-image differences by transforming linear combinations of band data into components that account for the maximum (first component) and successively lower proportions (second and higher order components) of variance among images. PCA was separately applied to a nine-band spectral data set (S-PCA), and a three-band data set comprised of NDVI data derived for each date (NDVI-PCA). Selection of the two PCA approaches was based on their potential for isolating changes due to flooding and similarity to methods employed in previous change-detection studies. Finally, differences in NDVI values observed prior to and following the flood (image differencing) were used in an unsupervised classification (NDVI-ID). Unless stated otherwise, standard default values were employed throughout the image rectification, normalization, and classification processes. Additional details related to method development, underlying conceptual and statistical assumptions, and performance expectations are discussed below.

Spectral-Temporal Change Classification

The basic premise for S-TCC is that spectral data for multi-date composite data sets would be similar in areas of no change, but would be significantly different statistically in areas experiencing change (Weismiller *et al.*, 1977). Potential disadvantages of the method include (1) redundancy in spectral information present in some of the bands, (2) difficulty in labeling change classes, and (3) relatively poor performance in previous studies (Weismiller *et al.*, 1977; Muchoney and Haack, 1994).

S-TCC was based on unsupervised classification of a merged 9-band data set containing spectral data for the three dates. An Iterative Self-Organizing Data Analysis technique (ISODATA; Tou and Gonzalez, 1974) was used in the unsupervised classification to generate 50 classes. This algorithm made multiple passes through the data, classifying pixels and updating cluster means, until cluster means did not change significantly with additional passes (Richards, 1986). Spectral classes were visually inspected and re-classed as flooded or non-flooded based on their appearance in the digital imagery, knowledge of the study area, and field and aerial surveys of flood-affected areas.

NDVI-Temporal Change Classification

The conceptual basis and potential disadvantages of this method are similar to those identified for S-TCC. Numerous studies have demonstrated that vegetation biomass and condition are often correlated with NDVI and other vegetation indices (Malingreau, 1989; Sader *et al.*, 1989; Vogelmann, 1990; Hunt, 1994; Gamon *et al.*, 1995; Nilsson, 1995). On this basis, we hypothesized that information present in the red and infrared bands would be most directly related to vegetation change and that classification accuracy might be expected to improve by focusing on NDVI-transformed data.

The NDVI-TCC technique was similar to S-TCC except that a three-band data set containing an NDVI image for each date was used in the unsupervised classification. NDVI values were transformed to 8-bit digital numbers (DNs) prior to subsequent analysis (Jensen, 1986).

Principal Components Analysis

Because of the high correlation in spectral information that is present in multi-date images, PCA has been used to transform the data into new images containing bands that are entirely uncorrelated. The basic premise for PCA in change detection is that one or more of the new PCA bands contains information that can be directly related to change (Byrne *et al.*, 1980; Jensen, 1986; Dobson *et al.*, 1995a). Muchoney and Haack (1994), for example, demonstrated that multitemporal SPOT spectral information related to hardwood defoliation by gypsy moths was confined to a single PCA band (3). In their study, PCA offered significant improvements in classification accuracy over S-TCC. Like S-TCC, however, it is often difficult to label change classes and from-to change class information is not available (Muchoney and Haack, 1994; Dobson *et al.*, 1995a).

Two PCA approaches were developed. The first approach, spectral PCA (S-PCA), was based on the merged nine-band data set containing all spectral bands from the three images. Analysis of the eigenstructure of the transformed data and visual inspection of eigenimages indicated that five components (3, 4, 6, 8, and 9), accounting for approximately 28 percent of the spectral variability among the images, best represented differences between 1994 and the other two image dates (Table 2). Components 3 and 4 were attributed to inter-image differences among the infrared (IR) bands that could be associated with vegetation responses to the relatively drier conditions in 1986 (especially PCA3), the flood in 1994 (especially PCA4), and other changes in vegetation cover. Components 6, 8, and 9 contrasted spectral variability in the red and green bands among the three images and were also retained for unsupervised classification. Components 1 and 2, which were related to overall brightness in the IR (PCA1) and green and red bands (PCA2), as well as components 5 and 7, which primarily highlighted differences in the red and green bands for the 1986 and 1990 imagery, were excluded from further analysis. We hypothesized that classification accuracy would be improved over the two temporal change classification techniques by focusing analysis on a subset of the most relevant uncorrelated data.

The second approach, NDVI-PCA, was based on the merged three-band data set consisting of NDVI images for each of the three dates. Like NDVI-TCC, we hypothesized that spectral information most directly related to vegetation change would be highlighted by focusing on NDVI-transformed data. The eigenstructure of the transformed data indicated that the first principal component (PCA1) was related to overall brightness of the three NDVI bands with similar loadings for the three images. PCA2 highlighted differences between 1994 and pre-flood conditions (1986 and 1990), and PCA3 was attributed primarily to differences between 1986 and 1990, although band loadings were dissimilar for the

TABLE 2. EIGENSTRUCTURE FOR MULTITEMPORAL PCS BASED ON SPECTRAL DATA

Year/Band	1	2	3	4	5	6	7	8	9
86 1	0.13	0.24	0.15	0.00	0.50	−0.01	−0.65	−0.48	0.06
2	0.17	0.42	0.17	−0.00	0.65	−0.08	0.48	0.34	−0.03
3	0.52	−0.16	0.79	0.05	−0.26	0.00	0.01	0.03	0.00
90 1	0.16	0.39	−0.11	−0.20	−0.25	−0.19	−0.49	0.63	0.17
2	0.16	0.56	−0.09	−0.19	−0.38	−0.38	0.27	−0.49	−0.15
3	0.57	−0.33	−0.34	−0.64	0.15	0.12	0.06	−0.05	−0.02
94 1	0.07	0.22	−0.04	0.06	−0.08	0.50	−0.13	0.10	−0.81
2	0.07	0.34	−0.03	0.00	−0.16	0.73	0.14	−0.12	0.53
3	0.55	−0.04	−0.42	0.71	−0.02	−0.09	−0.00	−0.00	0.05
Eigenvalues	57.47	43.13	23.74	12.60	10.08	5.28	1.10	0.72	0.35
% Variance	37.16	27.92	15.37	8.16	6.53	3.42	0.71	0.47	0.26
% Cumulative Variance	37.16	65.08	80.45	88.61	95.14	98.56	99.27	99.74	100.00

three image dates (Table 3). In this case, components 2 and 3 were retained for unsupervised classification which followed the S-TCC procedures that were previously described.

NDVI-Image Differencing

NDVI-ID is a technique whereby changes in NDVI values between two image dates are derived by cell-by-cell subtraction of co-registered data sets. The basic premise for image differencing is that subtraction results in an image data set where values less than or greater than zero indicate areas of change (Jensen, 1986; Dobson *et al.*, 1995a). Image differencing is computationally simple, and threshold values can be easily modified for classification improvement (Muchoney and Haack, 1994). When used with all image bands, however, image differencing provides no information on the nature of change (i.e., from-to classes) and interpretation can be difficult (Dobson *et al.*, 1995a). Interpretability could potentially be facilitated by transforming raw spectral data to an appropriate ratio or index that may be correlated with a specific type of change. For example, decreases in albedo obtained by multi-date image differencing have been used to identify arid areas that may have undergone desertification or site degradation (Robinove *et al.*, 1981).

In this study, 1994 NDVI values were subtracted from the 1986 and 1990 NDVI values separately and averaged to obtain a single value for each pixel that represents a magnitude and direction of change. In the resulting image data set, values that are negative or close to zero indicate areas where NDVI increased in 1994 or remained relatively unchanged, whereas positive values represent areas exhibiting a decrease in NDVI in 1994. A critical element in image differencing change detection is defining threshold values that indicate where significant change has occurred (Dobson *et al.*, 1995a). Frequently, a standard deviation from the mean is established as the threshold value (Jensen, 1986). In other cases, a threshold value representing a "realistic amount of change" is empirically selected after examining histograms of DN values (Dobson *et al.*, 1995a). Several alternative threshold values were examined in this study. A +1 SD (>9 DN) was selected as the threshold value because the resulting classification appeared reasonable based on knowledge of the study area and observations made during field and aerial surveys. We hypothesized that image differencing, like PCA, would result in improved classification accuracy over the temporal change classification methods, but that the results would be more easily interpreted than those obtained using PCA.

Accuracy Assessment

Data from 112 ground survey sites were used in the accuracy assessment. GPS-derived coordinates for each of the ground survey sites were used to relate ground-cover mortality data to specific flood zones, as well as binary flood classes generated from the five different change-detection methods (binary masks where 1 = flood). Sites were classified as live or dead based on the percentage ground cover dead (≥ 40% = dead). The number of dead sites classified as flooded versus those incorrectly classified as non-flooded, and the number of live sites classified as non-flooded versus those incorrectly classified as flooded, were used as a measure of how well each of the change detection methods performed. Overall accuracy and Kappa Coefficients (K_{hat}) were calculated for each method using techniques described by Congalton *et al.* (1983) and Congalton (1991). Two additional techniques, logistic multiple regression and a probability vector model, were used to quantitatively and visually compare the five change-detection methods. The quality of any accuracy assessment may be affected to varying degrees by unavoidable subjective analyst input. The methods employed in this study inherently required analyst input, and significant attention was devoted to minimizing analyst subjectivity by maintaining consistent classification and accuracy assessment methods whenever possible.

Logistic Multiple Regression

Logistic multiple regression was used to ascertain whether the five change-detection methods discriminated among sites based on overall site characteristics that might differentially respond to the severity of flooding (erosion, litter and sand deposition or removal, vegetation condition, and other factors that may vary by flood zone) or whether the methods were primarily sensitive to the proportion of live or dead ground-cover vegetation. Logistic regression has been used in many scientific disciplines to investigate the relationship between response probabilities of binary and ordinal response variables, and the explanatory variables (Hosmer and Lemeshow, 1989). The logistic model has the form

$$\text{logit}(\rho) = \log(\rho/(1 - \rho)) = \alpha + \beta' X,$$

where α is the intercept, β is the set of slope parameters associated with the independent predictor variables, and ρ is the probability that the response (Y) is "1" given a vector of

TABLE 3. EIGENSTRUCTURE FOR MULTITEMPORAL PCS BASED ON NDVI DATA

Band	1	2	3
86	0.50	−0.41	0.76
90	0.70	−0.33	−0.64
94	0.51	0.85	0.12
Eigenvalues	346.06	67.54	40.97
% Variance	76.13	14.86	9.01

explanatory variables (i.e., $p = \Pr(Y = 1 \mid X)$). The binary response variable was defined as flooded (1) or non-flooded (0) and varied for the different change-detection techniques. Predictor variables included percent live ground cover, percent dead ground cover, and flood zone. A stepwise selection procedure was employed using the SAS LOGISTIC procedure (SAS Institute, Inc., 1989).

Probability Vector Model

A probability vector model (PVM) was used to facilitate visualization of accuracy assessment for the five classification schemes. PVM represents a general error model that was developed by Goodchild *et al.* (1992) for obtaining estimates of uncertainty in land-cover maps. In their model, each classification scheme is treated as a "realization" and combined to form a data layer from which the uncertainty associated with a class at any point (or pixel, ij) is represented by a vector of probabilities $\{p_{ij1}, p_{ij2}, \ldots, p_{ijn}\}$ defining the probability that a pixel belongs to each class 1 through n (Goodchild *et al.*, 1992; Goodchild, 1994). Maps derived from probability vector modeling can be used to visually interpret classifications resulting from multiple change-detection methods and may enhance understanding of factors that affect accuracy. For example, large areas that are similarly classified by all or most methods can be readily identified. Areas of disagreement (lower probability scores) may indicate mixed pixels or class uncertainty. In addition, changes occurring in a particular land-cover class (e.g., vegetation senescence) that are being confused with the change of interest (e.g., flood-affected vegetation) may be visually interpreted.

In this study, the five different binary images were combined to derive probability values that ranged from 0 to 1, representing the proportion of times a pixel was classified as flooded by the different methods or realizations. Thus, a probability value equal to 0.6 indicates that the pixel was classified as flooded by three of the five techniques. For the area outside of the flood boundary, probability values derived from the PVM were then combined with land cover data for several forest community types to assess sources of confusion in the classification process.

Results

Overall accuracy and Kappa Coefficient statistics (K_{hat}) were used to compare the different change-detection techniques (Table 4). Overall accuracy for the techniques ranged from 0.607 to 0.768. However, K_{hat}, which indicates the degree of improvement over a random classification (0 representing chance alone; 1 indicating complete agreement), exhibited significant variation, ranging from 0.248 to 0.507. Both measures indicated that spectral-temporal change classification was least effective in discriminating flood-affected vegetation (Table 4a; Figure 2a).

Classification accuracy was improved when temporal change classification was based on NDVI data for the three dates (Table 4b; Figure 2b). In contrast, classification accuracy (K_{hat}) of PCA was only slightly higher when NDVI data (Table 4d; Figure 2d) were used instead of the original nine spectral bands (Table 4c; Figure 2c). Both PCA methods offered improved classification accuracy over the temporal change classification methods (S-TCC and NDVI-TCC). NDVI image differencing was the most effective technique for discriminating vegetation responses to flooding (Table 4e; Figure 2e). Examination of the NDVI data indicated that DNs were consistently lower (−10 DNs) in both flooded and non-flooded areas in 1986, the drier year, in comparison to 1990 (Table 5). In contrast, post-flood (1994) NDVI values in the non-flooded area approximated those observed in 1990, whereas those in the flooded area exhibited a 10-DN decrease. These findings indicate that ground cover vegetation exhibits a marked spectral response to both flooding and dry conditions which can be detected as a decrease in NDVI in affected areas.

TABLE 4. ACCURACY ASSESSMENT OF FIVE CHANGE-DETECTION TECHNIQUES USED TO ASSESS VEGETATION RESPONSES TO FLOODING

Method	No. Dead Sites		No. Live Sites			
	Correct	Incorrect	Correct	Incorrect	Accuracy	K_{hat}
(a) S-TCC	36	10	32	34	0.607	0.248
(b) NDVI-TCC	38	8	37	29	0.670	0.362
(c) S-PCA	33	13	46	20	0.705	0.405
(d) NDVI-PCA	41	5	37	29	0.696	0.419
(e) NDVI-ID	29	17	57	9	0.768	0.507

Logistic multiple regression results indicated that all methods were sensitive to the amount of dead vegetation present in the reference plots (Table 6). NDVI image differencing was the only method that was also affected by the presence of live vegetation (Table 6e). NDVI-TCC was the only method where results were also related to the flood duration zone (Table 6b). Classifications based on the image differencing technique exhibited the highest agreement (concordance represents the correlation between the predicted probabilities and observed binary responses) with the reference data (Table 6e).

Based on PVM, it was possible to visualize the degree of agreement among the techniques in identifying vegetation changes within the flood zone (Plate 2). Most (81 percent) of the forested area within the flood boundary was classified as flooded by one or more of the five change detection methods ($P \geq 0.2$). Within the flood boundary, 80 percent of the area classified as flooded was identified by at least two of the five techniques ($P \geq 0.4$) and 38 percent of the area was discriminated by at least four of the five techniques ($P \geq 0.8$). Flood-affected vegetation along the Flint River and Ichawaynochaway Creek that was identified by all five techniques ($P = 1.0$) represented 20 percent of the area within the flood boundary and generally occurred in areas that experienced highest current velocities and deepest waters as well as in localized depressions where standing water remained for several days following the flood.

In contrast, 44 percent of the area occurring outside the flood boundary was classified as flooded by one or more of the five change-detection techniques ($P \geq 0.2$). However, almost half (47 percent) of the area outside the flood boundary that was classified as flooded was discriminated only once by one of the five techniques. Only 4 percent of the area outside the flood boundary that was classified as flooded was identified by all five techniques ($P = 1.0$). Examination of classification "errors" outside the flood boundary indicated that pixels comprising certain forest types were more likely to be classified as flooded than others. For example, pixels occupied by cypress wetlands and deciduous xeric communities were especially prone to being classified as flooded by four or more of the change detection methods. In addition, there was a positive relationship between susceptibility to being classified as flooded by at least two of the methods and the proportion of the community comprised of deciduous trees (e.g., deciduous > mixed pine/hardwood > pine).

Discussion

Satellite data have been used to reconstruct regional flood history (Nagarajan *et al.*, 1993) and map water boundaries and changes in major wetland habitat types (Wickware and Howarth, 1981; Walsh and Townsend, 1995). Although a few studies have related agricultural crop damage to severity of flooding (Yamagata and Akiyama, 1988; Yamagata *et al.*, 1988), none have related ground-cover vegetation responses to

flooding in natural terrestrial ecosystems. Several factors might be expected to constrain flood impact assessments. First, due to overflight schedules and cloudiness, the timing of satellite data coverages rarely coincides with peak flood conditions, thereby leading to underestimates of the severity and areal extent of flood inundation (Blasco *et al.*, 1992). Second, dense vegetation canopy and the complex relationship between hydrologic and phenologic cycles may confound vegetation spectral responses within the floodplain (Walsh and Townsend, 1995). Third, accuracy assessments generally require reliable post-flood ground truth data, adequate digital elevation models, or other data that are often lacking or inadequate. Finally, vegetation may exhibit a lagged response to secondary flood-related factors (anaerobiasis, waterlogging, etc.) in areas that do not directly experience the most intense erosion and scouring (Craighead, 1971).

TABLE 5. MEAN NDVI VALUES FOR THE 1986, 1990, AND 1994 SPOT XS DATA

Image Date	Entire Site	Non-flooded	Flooded	Standard Deviation
18 Oct 86	180.2	179.8	182.0	1.6
5 Oct 90	190.2	189.7	192.5	1.9
28 Sep 94	186.4	187.6	181.7	4.1

In this study, cloud-free satellite data could not be acquired until almost three months after the flood. Relatively sparse overstory canopy coupled with a dense ground-cover community primarily dominated by a single species (wiregrass) characterized the study area and facilitated change-detection analyses. Classification accuracy exceeded 60 percent

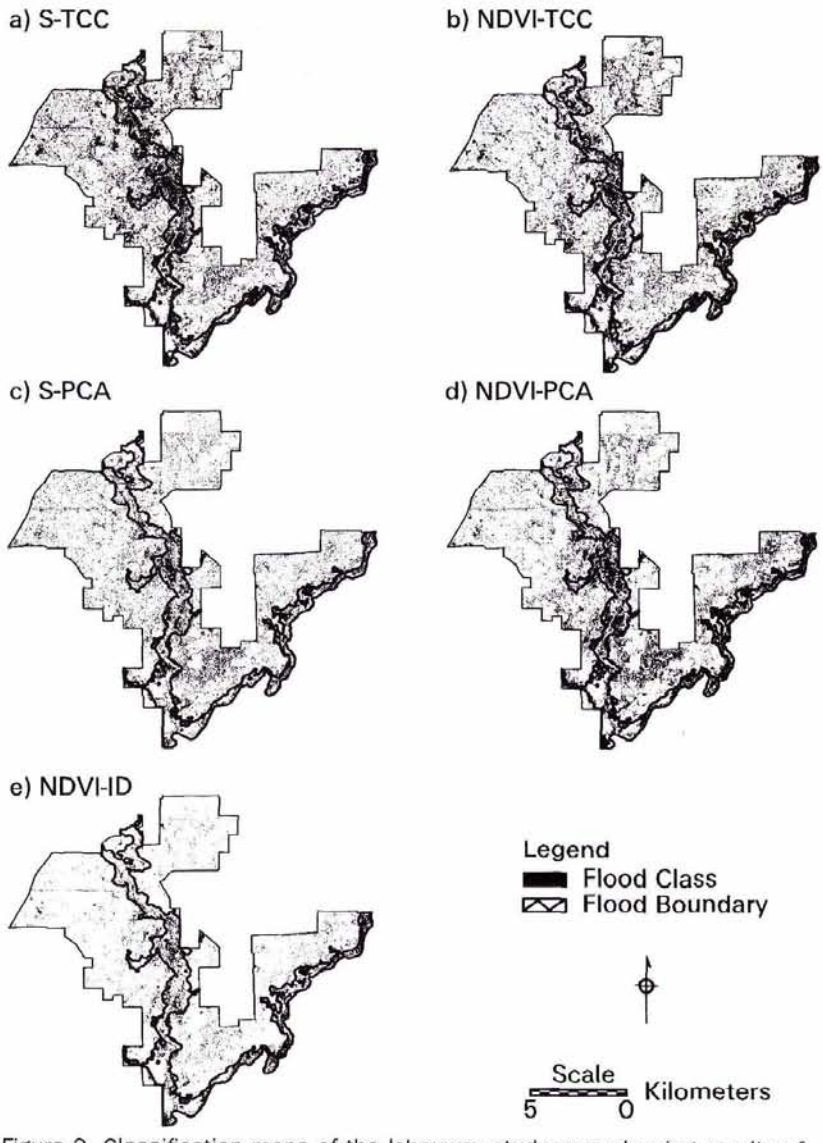

Figure 2. Classification maps of the Ichauway study area showing results of change-detection analyses based on (a) spectral-temporal change classification (S-TCC), (b) temporal change classification based on Normalized Difference Vegetation Index data (NDVI-TCC), (c) principal components analysis based on all spectral bands (S-PCA), (d) PCA based on NDVI data (NDVI-PCA), and (e) image differencing of NDVI data using +1 standard deviation as a threshold (NDVI-ID).

TABLE 6. LOGISTIC REGRESSION RESULTS COMPARING THE PREDICTION CAPABILITY OF THE CHANGE-DETECTION METHODS WITH THE PERCENT DEAD AND LIVE GROUND COVER, AND THE FLOOD ZONE

	Chi-square Test of Significance (P-value)			Measure of Model Predictive Capability		
Method	% Dead	% Live	Flood Zone	% Concordance	% Discordance	% Tied
(a) S-TCC	0.0007	>0.05	>0.05	68.1	28.9	3.1
(b) NDVI-TCC	0.0010	>0.05	0.0271	74.9	24.4	0.7
(c) S-PCA	0.0001	>0.05	>0.05	71.3	27.1	1.6
(d) NDVI-PCA	0.0001	>0.05	>0.05	76.0	21.9	2.1
(e) NDVI-ID	0.0001	0.0347	>0.05	82.3	16.9	0.9

for the five methods used in this study, suggesting that all techniques offered potential for discriminating vegetation responses to flooding. Although accuracy of the various classification methods employed in this study may limit their utility for management applications, the two-fold range in Kappa Coefficient Statistics (K_{hat} = 0.248 − 0.507) indicated that some methods outperformed others when chance agreement was removed. Specifically, it is possible to generalize that (1) temporal change classification based on changes in NDVI were more accurate than similar classifications based on changes occurring in all spectral bands, (2) PCA techniques (S-PCA and NDVI-PCA) resulted in increased classification accuracy over the temporal change classification methods, and (3) image differencing of NDVI data represented the most effective method for discriminating flood-affected vegetation.

Results obtained in this and previous studies may facilitate the selection of appropriate methods for discriminating change in different ecosystems resulting from different types and magnitude of disturbance. First, disadvantages associated with S-TCC, including poor classification accuracy in this and previous studies (e.g., Muchoney and Haack, 1994), may reduce the utility of this method for detecting environmental change. Despite the improvement in classification accuracy when TCC was based on NDVI data, the high degree of correlation among both spectral bands and vegetation indices (e.g., NDVI) for multiple dates (collinearity) may have deleterious effects on classification accuracy and may violate assumptions of many statistical tests. Second, although PCA offered improvements in classification accuracy over the two temporal change classification methods, interpretation was not straightforward and required extensive knowledge of the study area. One interesting outcome of the study was the similarity in classification accuracy between the S-PCA and NDVI-PCA, which suggested that minimal benefits may be derived by transforming data from a relatively small number of images prior to PCA. However, appropriate indices may be useful when large numbers of images are included in PCA. Third, image differencing of NDVI data provided the highest accuracy and is a relatively straightforward technique that could be automated for long-term monitoring of environmental change. In this study, statistically significant spectral changes were correlated with ecologically significant vegetation changes that occurred

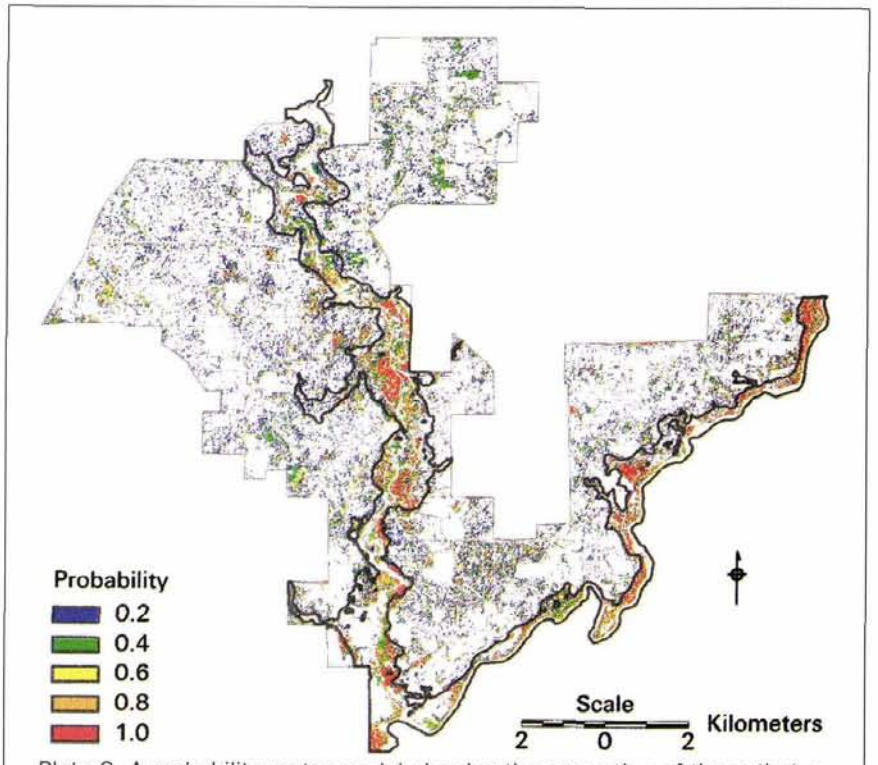

Plate 2. A probability vector model showing the proportion of times that a pixel was classified as flooded by the five different change-detection techniques.

in flood-affected areas and results could be readily interpreted. Muchoney and Haack (1994) observed that image differencing of SPOT XS bands was the most accurate of the four change-detection approaches they used for identifying hardwood forest defoliation caused by gypsy moth infestation. However, like PCA, interpretation of spectral image differencing results may be difficult, whereas the use of meaningful indices, such as NDVI, may facilitate interpretation of change images.

Automated change detection requires that baseline conditions be defined prior to assessment of change. In this study, accurate results were obtained when baseline conditions reflected the typical range in precipitation that is observed during the fall season (normal to dry). Once baseline conditions are established and change is detected in a new satellite image, ground- or aerial-photography-based assessments are essential for determining whether "significant" spectral change, as defined by the change threshold, is ecologically meaningful. One interesting outcome of the logistic multiple regression analysis of the ground survey data was the sensitivity of all change-detection methods to the percentage of dead ground cover, a relatively simple measure of vegetation condition that can be easily assessed in the field. The lack of a strong and consistent relationship between flood zone and the predictive capabilities of the change-detection methods may be related to soil, physiographic (slope, aspect, etc.), and other site-specific factors that varied considerably within the designated flood zones, thereby affecting the magnitude of the disturbance (depth, duration, intensity) experienced by the vegetation.

PVM proved useful for visually assessing classification accuracy and identifying potential sources of confusion. The tendency for pixels located in cypress wetlands and deciduous xeric communities located outside of the flood boundary to be more frequently classified as flooded than were other forest types was unexpected. However, at least two mechanisms may account for this phenomena. First, the two habitats comprise a total of only 161 ha and consist of many small patches that are scattered throughout the landscape. Some misclassification associated with mixed pixels might, therefore, be expected based solely upon patch morphology. Second, spectral changes associated with these habitats may reflect vegetation changes that occurred in response to excessive precipitation. Standing water was observed in cypress wetlands for an extended period following Tropical Storm Alberto and likely had an adverse effect on ground-cover vegetation. Similarly, extended soil saturation of deciduous xeric habitats may have resulted in root stress and enhanced denitrification rates, and concomitant negative effects on aboveground vegetation biomass and condition (Craighead, 1971; R. Mitchell, personal communication). Because ground-cover vegetation was not sampled in either habitat, it would be inappropriate to assume that pixels in the two habitats represented misclassification errors instead of actual biological responses to the disturbance.

Logistic multiple regression and PVM represent powerful analytical techniques that may prove useful in other evaluations of change-detection methods. Binary response variables (e.g., defoliated, unaffected) and ordinal response variables (e.g., no effect, moderate defoliation, severe defoliation) arise in many studies of ecological disturbances. Logistic regression analysis can be effectively used to investigate the relationship between the spectrally defined response probability and potential explanatory variables (e.g., degree of canopy closure, stand condition, etc.). Results of such analyses could be used to reduce the number of attributes that are monitored in the field, thereby reducing sampling costs.

Maps derived from probability vector modeling may facilitate visual assessments of classification accuracy when comparing multiple methods, allowing the analyst to identify areas of agreement and disagreement. Areas susceptible to misclassification may be easily visualized, interpreted, and corrected. Such sources of confusion may not be readily apparent using standard classification accuracy assessment techniques, especially if the researchers do not have extensive experience and/or knowledge of conditions on the ground. Goodchild *et al.* (1992) further discuss how this modeling approach can be used to obtain standard errors associated with area estimates.

Conclusion

Previous change-detection studies have primarily focused on applying a single change-detection technique for assessing vegetation changes related to alterations in land use (e.g., deforestation) and broad-scale natural disturbances (e.g., hurricanes, drought, insect outbreaks). This study demonstrated the feasibility of using satellite data and different change-detection approaches to assess and monitor responses in ground-cover vegetation dynamics to flooding of a sparse canopy forested ecosystem. Two techniques utilized in this study, logistic multiple regression and PVM, were useful for relating spectral change to vegetation change and visualizing classification accuracy, and may facilitate future change-detection studies. Although additional comparative studies in a variety of ecosystems experiencing different types and intensity of disturbance are required, automated change detection offers significant potential for increasing our understanding of ecosystem- and landscape-scale responses to natural and anthropogenic disturbances.

Acknowledgments

We thank Don Edwards for assistance in data analysis; the numerous students and technicians who participated in ground survey efforts, especially Derek Fussell; Frank Miller, Mary Grace Chambers and Linda Garnett of the Mississippi Remote Sensing Center, and Jean Brock (JWJERC) for GIS support; and Marguerite Remillard, Don Edwards, and three anonymous reviewers for critical review of the manuscript. This project was funded by the National Science Foundation (DEB-9520878).

References

Aldrich, R.C., 1975. Detecting disturbances in a forest environment, *Photogrammetric Engineering & Remote Sensing*, 41:39–48.

Bauer, M.E., T.E. Burk, A.R. Ek, P.R. Coppin, S.D. Lime, T.A. Walsh, D.K. Walters, W. Befort, and D.F. Heinzen, 1994. Satellite inventory of Minnesota forest resources, *Photogrammetric Engineering & Remote Sensing*, 60(3):287–298.

Blasco, F., M.F. Bellan, and M.U. Chaudhury, 1992. Estimating the extent of floods in Bangladesh using SPOT data, *Remote Sensing of Environment*, 39:167–178.

Byrne, G.F., P.F. Crapper, and K.K. Mayo, 1980. Monitoring land-cover change by principal component analysis of multitemporal Landsat data, *Remote Sensing of Environment*, 10:175–184.

Cablk, M.E., B. Kjerfve, W.K. Michener, and J.R. Jensen, 1994. Impacts of Hurricane Hugo on a coastal forest: Assessment using Landsat TM data, *Geocarto International*, 2:15–24.

Caselles, V., and M.J. Lopez Garcia, 1989. An alternative simple approach to estimate atmospheric correction in multitemporal studies, *International Journal of Remote Sensing*, 10(6):1127–1134.

Chavez, P.S., and D.J. MacKinnon, 1994. Automatic detection of vegetation changes in the southwestern U.S. using remotely sensed images, *Photogrammetric Engineering & Remote Sensing*, 60(5): 571–583.

Cohen, W.B., J.D. Kushla, W.J. Ripple, and S.L. Garman, 1996. An introduction to digital methods in remote sensing of forested ecosystems: Focus on the Pacific Northwest, USA, *Environmental Management*, 20(3):421–435.

Collins, J.B., and C.E. Woodcock, 1996. An assessment of several linear change detection techniques for mapping forest mortality us-

ing multitemporal Landsat TM data, *Remote Sensing of Environment*, 56:66–77.

Congalton, R.G., 1991. A review of assessing the accuracy of classifications of remotely sensed data, *Remote Sensing of Environment*, 37:35–46.

Congalton, R.G., R.G. Oderwald, and R.A. Mead, 1983. Assessing Landsat classification accuracy using discrete multivariate analysis statistical techniques, *Photogrammetric Engineering & Remote Sensing*, 49(12):1671–1678.

Craighead, F.C., 1971. *The Trees of South Florida, Vol. 1, The Natural Environments and Their Succession*, University of Miami Press, Coral Gables, Florida.

Dobson, J.E., E.A. Bright, R.L. Ferguson, D.W. Field, L.L. Wood, K.D. Haddad, H.I. Iredale III, J.R. Jensen, V.V. Klemas, R.J. Orth, and J.P. Thomas, 1995a. *NOAA Coastwatch Change Analysis Program (C-CAP) Guidance for Regional Implementation*, NOAA Technical Report NMFS123, NOAA Coastal Ocean Program, U.S. Department of Commerce, Washington, D.C.

Dobson, E.L., J.R. Jensen, R.B. Lacy, and F.G. Smith, 1995b. A land cover characterization methodology for large area inventories, *ACSM/ASPRS Proceedings*, Charlotte, North Carolina, pp. 786–795.

Eckhardt, D.W., J.P. Verdin, and G.R. Lyford, 1990. Automated update of an irrigated land GIS using SPOT HRV imagery, *Photogrammetric Engineering & Remote Sensing*, 56(11):1515–1522.

Ferencz, C., G. Tarcsai, and J. Lichtenberger, 1993. Correction of atmospheric effects of satellite remote sensing data (Landsat MSS, NOAA AVHRR) for surface canopy investigations, *International Journal of Remote Sensing*, 14(18):3417–3431.

Foody, G.M., and P.J. Curran, 1994. Estimation of tropical forest extent and regenerative stage using remotely sensed data, *Journal of Biogeography*, 21:223–244.

Gamon, J.A., C.B. Field, M.L. Goulden, K.L. Griffin, A.E. Hartley, G. Joel, J. Penuelas, and R. Valentini, 1995. Relationship between NDVI, canopy structure, and photosynthesis in three Californian vegetation types, *Ecological Applications*, 5(1):28–41.

Garza, C., 1995. Alberto: A hydrometeorologic nightmare, *Proceedings of the 1995 Georgia Water Resources Conference* (K.J. Hatcher, editor), University of Georgia, Athens, Georgia, pp. 310–312.

Goodchild, M.F., 1994. Integrating GIS and remote sensing for vegetation analysis and modeling: Methodological issues, *Journal of Vegetation Science*, 5:615–626.

Goodchild, M.F., G.Q. Sun, and S. Yang, 1992. Development and test of an error model for categorical data, *International Journal Geographic Information Systems*, 6:87–104.

Hall, F.G., D.E. Strebel, J.E. Nickeson, and S.J. Goetz, 1991. Radiometric reflection: Toward a common radiometric response among multidate multisensor images, *Remote Sensing of Environment*, 35:11–27.

Hosmer, D.W., and S. Lemeshow, 1989. *Applied Logistic Regression*, John Wiley and Sons, Inc., New York, N.Y.

Hunt, E.R., 1994. Relationship between woody biomass and PAR conversion efficiency for estimating net primary production from NDVI, *International Journal of Remote Sensing*, 15(8):1725–1730.

Jacobberger-Jellison, P.A., 1994. Detection of post-drought environmental conditions in the Tombouctou region, *International Journal of Remote Sensing*, 15(16):3138–3197.

Jensen, J.R., 1986. *Introductory Digital Image Processing*, Prentice-Hall, Englewood Cliffs, New Jersey.

Jensen, J.R., D. Cowen, J.D. Althausen, S. Narumalani, and O. Weatherbee, 1993. An evaluation of the CoastWatch change detection protocol in South Carolina, *Photogrammetric Engineering & Remote Sensing*, 59(6):1039–1046.

Jensen, J.R., K. Rutchey, M.S. Koch, and S. Narumalani, 1995. Inland wetland change detection in the Everglades Water Conservation Area 2A using a time series of normalized remotely sensed data, *Photogrammetric Engineering & Remote Sensing*, 61(2):199–209.

Johnson, R.D., 1994. Change vector analysis for disaster assessment: A case study of Hurricane Andrew, *Geocarto International*, 1:41–45.

Kim, H.H., and G.C. Elman, 1990. Normalization of satellite imagery, *International Journal of Remote Sensing*, 11(8):1331–1347.

Loope, L., M. Duever, A. Herndon, J. Snyder, and D. Jansen, 1994. Hurricane impact on uplands and freshwater swamp forest, *BioScience*, 44(4):238–246.

Malingreau, J.P., 1989. The vegetation index and the study of vegetation dynamics, *Applications of Remote Sensing to Agrometeorology* (F. Toselli, editor), Kluwer Academic Publishers, Dordrecht, The Netherlands, pp. 285–303.

Michener, W.K., E.R. Blood, K.R. Bildstein, M.M Brinson, L.R. Gardner, 1997. Climate change, hurricanes and tropical storms, and rising sea level in coastal wetlands: Projected ecological impacts and research challenges, *Ecological Applications*, 7(3):770–801.

Michener, W.K., E.R. Blood, S.W. Golladay, L.K. Kirkman, R.J. Mitchell, and B.J. Palik, 1995. Effects of flooding on the longleaf pine-wiregrass ecosystem, *Proceedings of the 1995 Georgia Water Resources Conference* (K.J. Hatcher, editor), University of Georgia, Athens, Georgia, pp. 190–193.

Muchoney, D.M., and B.N. Haack, 1994. Change detection for monitoring forest defoliation, *Photogrammetric Engineering & Remote Sensing*, 60(10):1243–1251.

Nagarajan, R., G.T. Marathe, and W.G. Collins, 1993. Identification of flood prone regions of Rapti river using temporal remotely-sensed data, *International Journal of Remote Sensing*, 14(7):1297–1303.

Nilsson, H.E., 1995. Remote sensing and image analysis in plant pathology, *Annual Review of Phytopathology*, 15:489–527.

Olsson, H., 1995. Reflectance calibration of TM data for forest change detection, *International Journal of Remote Sensing*, 16(1):81–96.

Peters, A.J., B.C. Reed, M.D. Eve, and K.M. Havstad, 1993. Satellite assessment of drought impact on native plant communities of Southeastern New Mexico, U.S.A., *Journal of Arid Environments*, 24:305–319.

Pickett, S.T.H., and P.S. White (editors), 1985. *The Ecology of Natural Disturbance and Patch Dynamics*, Academic Press, Orlando, Florida.

Price, J., 1987. Calibration of satellite radiometers and the comparison of vegetation indices, *Remote Sensing of Environment*, 21:15–27.

Richards, J.A., 1986. *Remote Sensing Digital Image Analysis*, Springer-Verlag, Heidelberg, Germany.

Robinove, C.J., P.S. Chavez, D. Gehring, and R. Holmgren, 1981. Arid land monitoring using Landsat albedo difference images, *Remote Sensing of Environment*, 11:133–156.

Sader, S.A., R.B. Waide, W.T. Lawrence, and A.T. Joyce, 1989. Tropical forest biomass and successional age class relationships to a vegetation index derived from Landsat TM data, *Remote Sensing of Environment*, 28:143–156.

SAS Institute, Inc., 1989. *SAS/STAT User's Guide*, Version 6, 4th Edition, Volume 2, SAS Institute, Inc., Cary, North Carolina.

Schott, J.R., C. Salvaggio, and W.J. Volchok, 1988. Radiometric scene normalization using pseudoinvariant features, *Remote Sensing of Environment*, 26:1–16.

Sirois, J., and F.J. Ahern, 1989. An investigation of SPOT HRV data for detecting recent mountain pine beetle mortality, *Canadian Journal of Remote Sensing*, 14(2):104–108.

Stamey, T.C., 1995. Floods in Central and Southwestern Georgia in July 1994, *Proceedings of the 1995 Georgia Water Resources Conference* (K.J. Hatcher, editor), University of Georgia, Athens, Georgia, pp. 313–316.

Tou, J.T., and R.C. Gonzalez, 1974. *Pattern Recognition and Principles*, Addison-Wesley Publishing Company, Reading, Massachusetts.

Vogelmann, J.E., 1988. Detection of forest change in the Green Mountains of Vermont using MSS data, *International Journal of Remote Sensing*, 9(7):1187–1200.

———, 1990. Comparison between two vegetation indices for measuring different types of forest damage in the north-eastern U.S, *International Journal of Remote Sensing*, 11(12):2281–2297.

Walsh, S.J., and P.A. Townsend, 1995. Comparison of change detection approaches for assessing a riverine flood hydroperiod, *ACSM/ASPRS Proceedings*, Charlotte, North Carolina, pp. 134–143.

Weismiller, R.A., S.J. Kristof, D.K. Scholz, P.E. Anuta, and S.M. Momin, 1977. Evaluation of change detection techniques for monitoring coastal zone environments, *Proceedings of the Eleventh International Symposium on Remote Sensing of Environment*, ERIM, Ann Arbor, Michigan.

Wickware, G.M., and P.J. Howarth, 1981. Change detection in the Peace-Athabasca Delta using digital Landsat data, *Remote Sensing of Environment*, 11:9–25.

Wolter, P.T., D.J. Mladenoff, G.E. Host, and T.R. Crow, 1995. Improved forest classification in the northern lake states using multi-temporal Landsat imagery, *Photogrammetric Engineering & Remote Sensing*, 61(9):1129–1143.

Yamagata, Y., and T. Akiyama, 1988. Flood damage analysis using multitemporal Landsat TM data, *International Journal of Remote Sensing*, 9(3):503–514.

Yamagata, Y., C. Wiegand, T. Akiyama, and M. Shibayama, 1988. Water turbidity and perpendicular vegetation indices for paddy rice flood damage analysis, *Remote Sensing of Environment*, 26:241–251.

(Received 20 March 1996; revised and accepted 15 January 1997; revised 11 March 1997)